Study of Multiple Scattering in Upstream Detectors in DIRAC

B. Adeva, A. Romero, O. Vázquez Doce

IGFAE, University of Santiago de Compostela, Spain

Abstract

In DIRAC, resolution in the $\pi^+\pi^-$ interaction vertex inside the target foil is dominated by multiple scattering in upstream spectrometer, including the target itself. A detailed analysis has been carried out of vertex resolution as function of momentum, where real 2001 spectrometer data have been compared with standard GEANT-DIRAC Monte Carlo simulation, including detector backgrounds. A significant discrepancy is found, which is unambiguously attributed to underestimation of average multiple scattering in upstream detectors by the Monte Carlo.

DIRAC internal note 2005 *3 October 2005*

1 Introduction

Knowledge of multiple scattering in DIRAC experiment is important because it determines Q resolution when Monte Carlo is used to extract the narrow signal from atom pairs. The upstream radiation length fraction is specially critical for Q_T resolution.

Chemical specifications, precise thicknesses and difficulty of very detailed geometry of components of SFD and MSGC detectors do not allow an "a priori" knowledge of the material contribution better that roughly 10%. Therefore measurements must be made with real data, in order to attain the percent accuracy level.

The four MSGC high resolution detectors placed at 1.5 m from the target foil, together with the GEANT tracking capability using Molière theory, provide a clean determination of multiple scattering fluctuations to this accuracy. Using tracking detectors to evaluate their own multiple scattering is the natural and standard way to do this job. The tracking tools were implemented in reference [1].

The obvious idea is to exploit the fact that real $\pi^+\pi^-$ prompt interactions come from a single mathematical space point (of nuclear size dimensions), and to use beam unconstrained track fitting to study the error.

2 Vertex resolution analysis

A vertex position has been defined inside the target plane by coordinates $(x_1 - x_2\ ,\ y_1 - y_2)$ where $x_{1,2}$ are extrapolated X-coordinates for positive and negative tracks (likewise for $y_{1,2}$) that pass the standard ARIANE reconstruction procedure, with full tracking. By taking the differences, the measurement becomes insensitive to fluctuations of track origin within the beam profile. Such fluctuations become uncorrelated only in the case of accidental pairs, where each track originates from an independent interaction.

In this analysis, we selected prompt pairs (by time-of-flight cut), in order to make sure that multiple scattering and, to a much lesser extent, detector resolution, are really the dominant contributions to the vertex error.

We made a gaussian fit to the vertex distributions in X and Y projections in 7 bins of track momentum, in the range from 1.5 GeV/c to 3.5 GeV/c. It is worth noting at this point that, as a standard part of the track fitting

procedure, far-away hits with respect to the track are removed by a 3σ cut. Only 6-hit track were retained for this analysis.

In order to make a meaningful comparision with the Monte Carlo with prompt pion production, a 10% fraction of the vertex distribution observed with accidental pairs has been subtrated at each momentum bin. This point will be discussed in more detail in section 3.5 below.

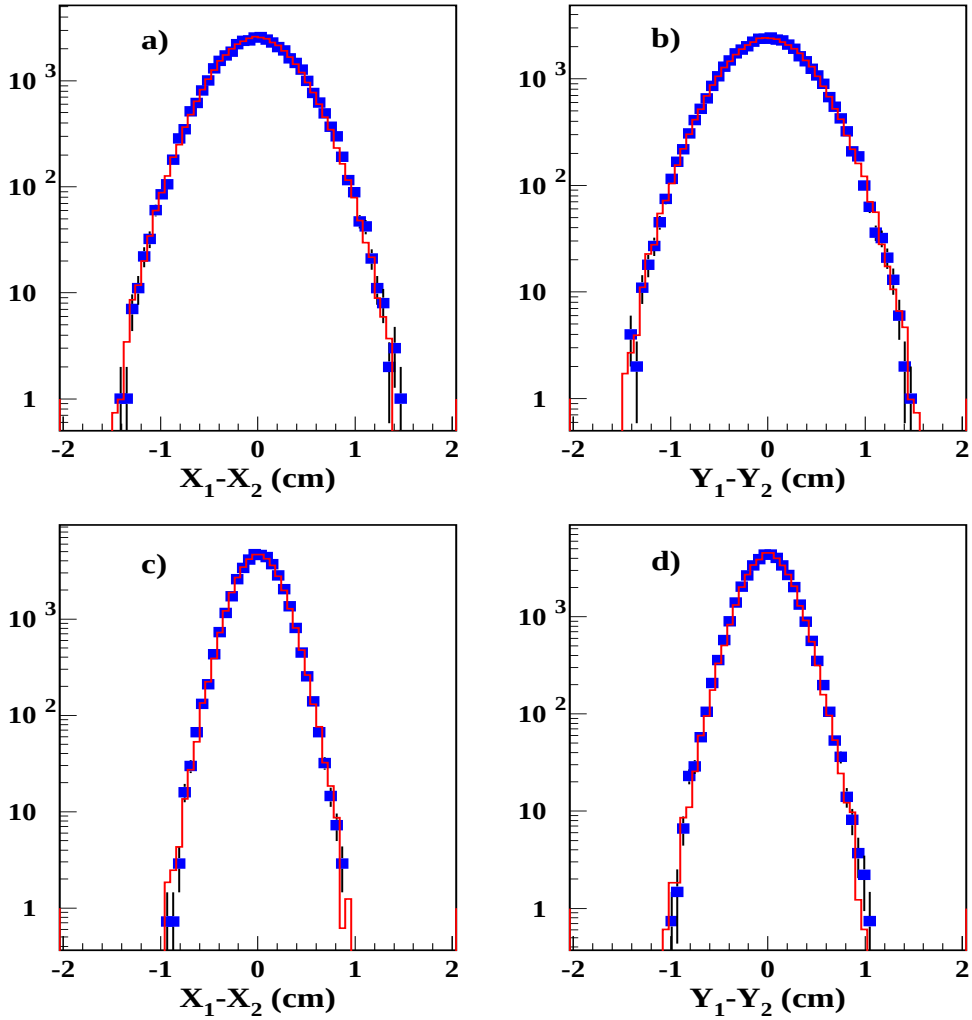

Fig. 1. *Vertex distributions in X and Y projections. Only the minimum ($p < 1.60 GeV/c$, top) , and maximum ($p > 3.25 GeV/c$, bottom) momentum bins of figure 2 are shown. GEANT Monte Carlo is superimposed for the optimum $\bar{\theta}_0$ found.*

The gaussian fit to the vertex distribution appears to be good in the central region, while small tails are observed at fixed momentum. These are a consequence of Coulomb large-angle scatters, as well as possible reminders from

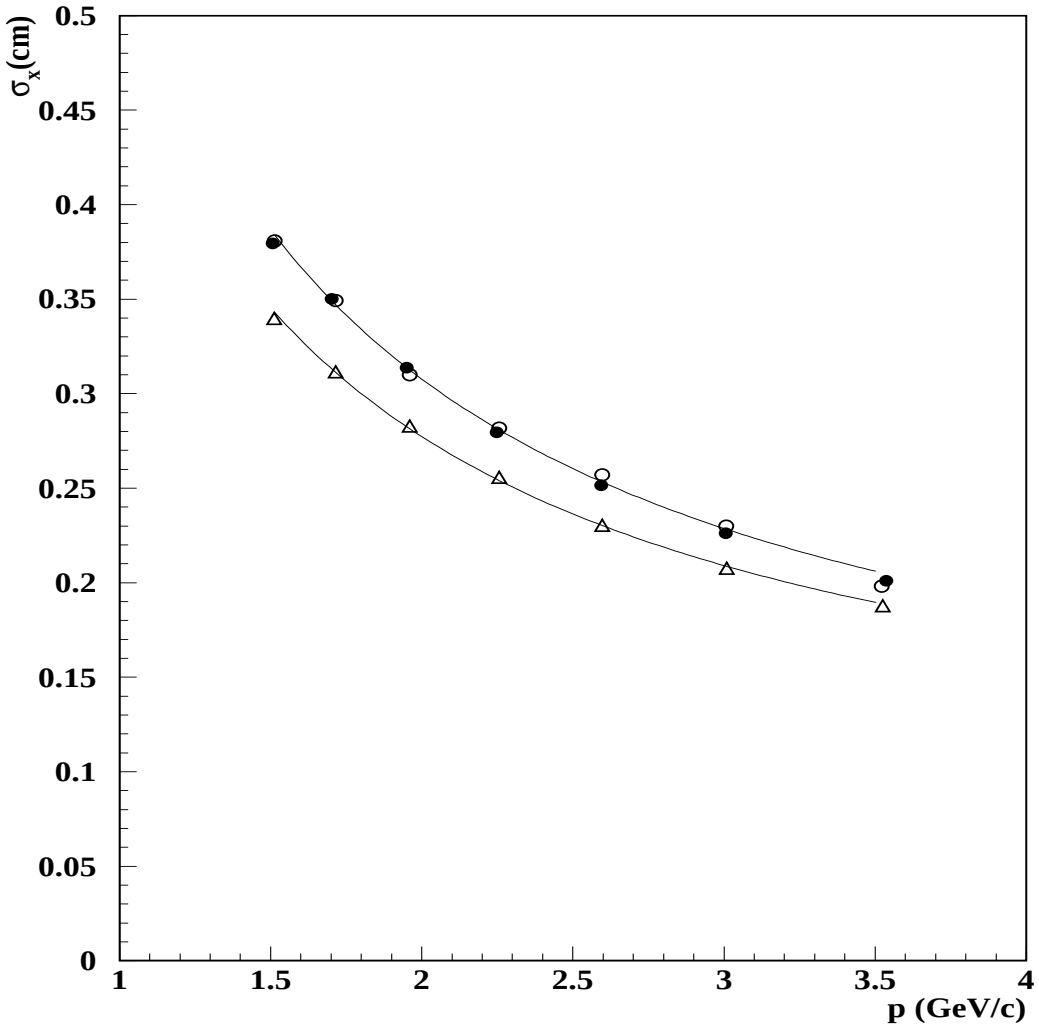

Fig. 2. *Vertex resolution in X-projection, as function of track momentum. Full circles are real prompt pairs (accidentals subtracted), and open circles the best Monte Carlo option illustrated in figure 4. Open triangles show the prediction from the standard GEANT-DIRAC, with material definition as in tables 1 and 2.*

accidentals and decays. The fits were consistently performed in the region $\pm 2\sigma$, in order to minimise the impact of the tails. For illustration, we show in figure 1 the vertex distributions in X and Y projections for the maximum and minimum momentum bins.

Please note that pattern recognition of individual tracks (which takes place prior to track fitting) requires the presence of MSGC and SFD hits within a pointing geometry with respect to the beam intersection with the target foil. Space windows used are explained in some detail in reference [1], and they are sized (analytically) in order to catch the interaction signal within aproximately

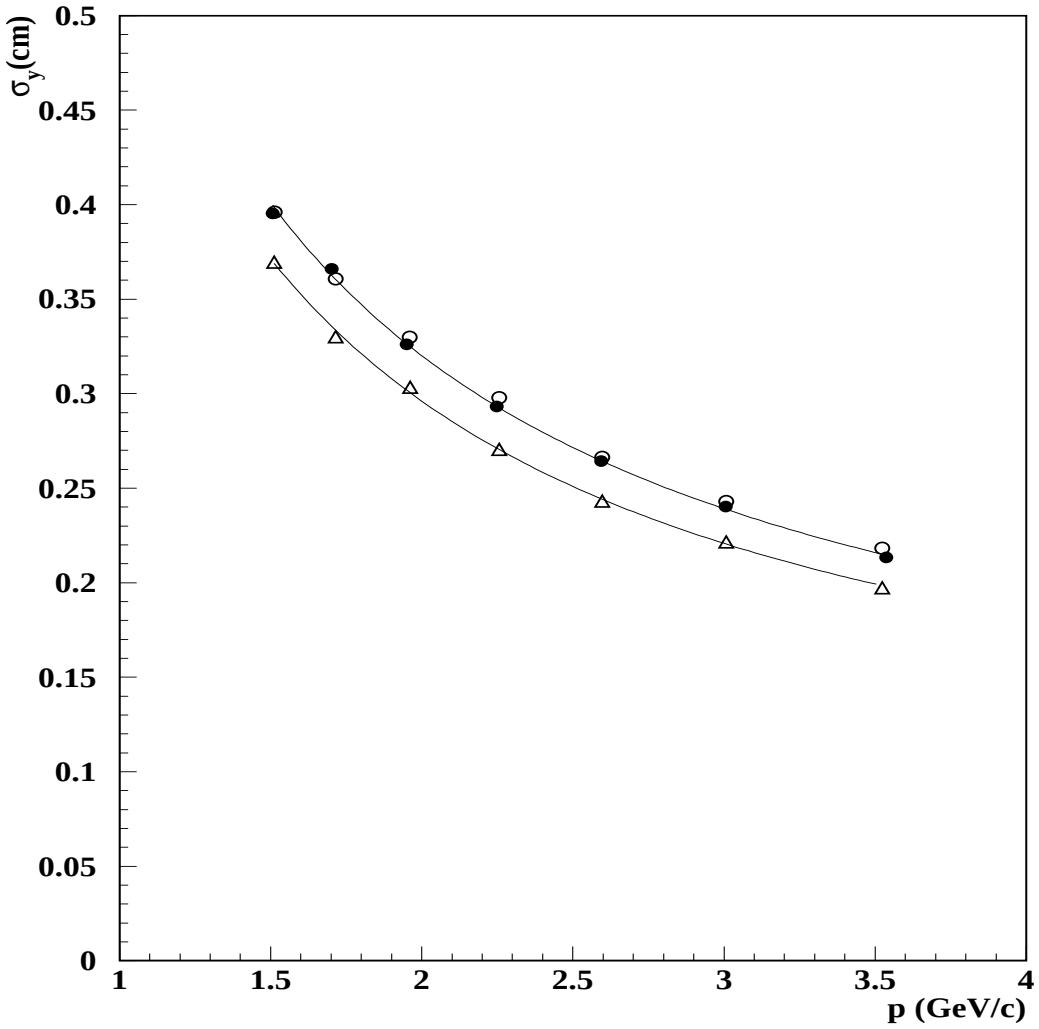

Fig. 3. *Vertex resolution in Y-projection, as function of track momentum. Full circles are real prompt pairs (accidentals subtracted), and open circles the best Monte Carlo option illustrated in figure 4. Open triangles show the prediction from the standard GEANT-DIRAC, with material definition as in tables 1 and 2.*

2.5σ from the predicted value, while removing at the same time decays and other background sources outside spotted region. This cut has been tightened for this study, for the reasons mentioned above.

We have calibrated the mean vertex position for different run periods in 2001, and found that its time dependence is strongly correlated with that observed from direct drift chamber alignment with respect to the beam. Although this is irrelevant for the difference $x_1 - x_2$, this calibration was indeed taken into account for track pattern recognition.

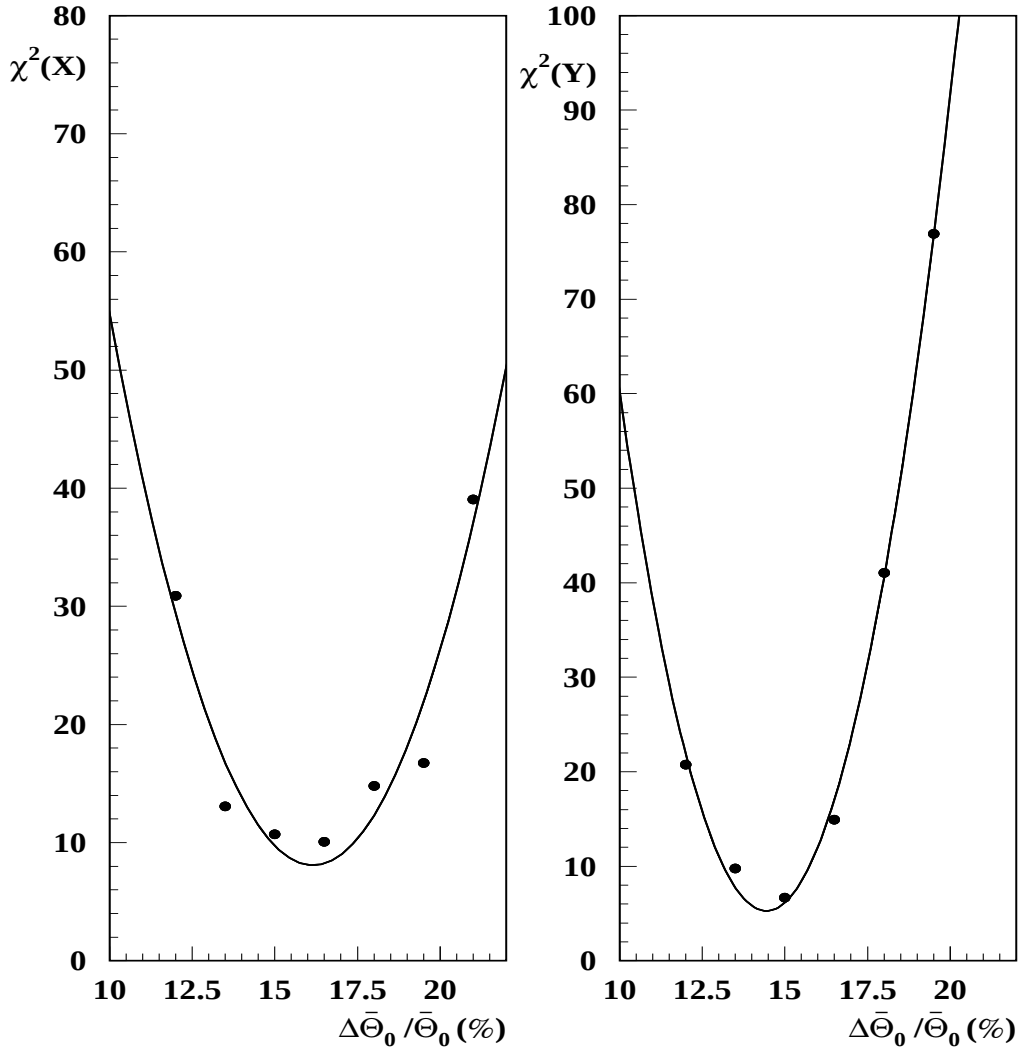

Fig. 4. χ^2 *between real data and Monte Carlo (as defined in the text) as function of increased average multiple scattering angle in upstream detectors, for X (left) and Y (right) projections. Only points near the minimum are shown.*

The evolution of fitted σ values with momentum, after subtraction of accidentals, is plotted in figures 2 and 3. These are called in the following vertex resolutions. Empirically, we have parametrised the momentum dependence of vertex resolution by the function $\sigma = a + b/p$, which provides an excellent description of the data.

Now the results obtained with the full 2001 24 GeV/c data sample (94μm Ni target) were compared with the GEANT-DIRAC Monte Carlo using standard geometry files, 94μm Ni target thickness, and specific material contributions for MSGC and SFD detectors as indicated in tables 1 and 2. The values of A,

Z, density ρ and thickness for each simulated material layer, which are the real input for GEANT-DIRAC, are given in the first four columns of this table.

It is important to recall here that the default version of GEANT program [2], (which is the one used by GEANT-DIRAC [3]), makes use of the Molière theory of multiple scattering, which operates at every step during the tracking, subject to the condition that the parameter Ω_0 is greater than 20. Ω_0 represents the number of scatters that take place in a given step length t, according to the expression:

$$\Omega_0 = b_c \frac{t}{\beta^2}$$

where

$$b_c = 6702.33 \rho Z_s^{'} e^{(Z_E^{'} - Z_X^{'}/Z_s^{'})}$$

with

$$Z_s^{'} = \sum_i \frac{p_i}{A_i} Z_i (Z_i + 1)$$

$$Z_E^{'} = \sum_i \frac{p_i}{A_i} Z_i (Z_i + 1) log {Z_i}^{-2/3}$$

$$Z_X^{'} = \sum_i \frac{p_i}{A_i} Z_i (Z_i + 1) log[1 + 3.34 (\frac{\alpha Z_i}{\beta})^2]$$

where p_i are the proportions by weight of atom type i with atom number Z_i and mass number A_i, within a compound made of $i = 1, N$ different elements. β is the particle velocity and α the fine structure constant.

Table 1
Tracking medium data used by standard GEANT-DIRAC for one generic MSGC detector. There are four identical planes.

Material	*A*	*Z*	$\rho(g/cm^3)$	$t = \Delta z$	$X_0(cm)$	$t/X_0(\times 10^{-4})$
DME	25.95	12.02	1.85×10^{-3}	0.200	14540.	0.138
DESAG($\times$2)	25.75	12.52	2.51	0.0231	9.877	23.39
Copper($\times$2)	63.54	29.00	8.96	0.00050	1.469	3.404
Kapton($\times$2)	12.70	6.36	1.42	0.00250	28.91	0.8647
Total						55.45$\times$4=221.8

Table 2
Tracking medium data used by GEANT-DIRAC for one SFD detector. There are two identical planes, X and Y (in 2001).

$Material$	A	Z	$\rho(g/cm^3)$	$t = \Delta z$	$X_0(cm)$	$t/X_0(\times 10^{-4})$
Polystyrene	11.16	5.61	1.032	0.250	43.55	57.40
Paint(×2)	18.08	8.77	1.26	0.01465	26.23	5.585
Cobex(×2)	13.94	6.90	1.35	0.022	28.91	7.609
Total						83.79×2=167.6

In the setup of DIRAC upstream detectors, the condition $\Omega_0 > 20$ is only violated (in a significant number of steps) in air gaps and MSGC DME gas, where GEANT is forced by the volume size to take a too small step size, in proportion with $1/\rho$. In those cases, a precise parametrisation is performed by GEANT, called plural scattering [2]. We do not enter here into a more detailed discussion of this part, because the impact of those cases in the overall scattering angle is, in any case, negligible.

More important is that the concept of radiation length X_0 [5], usually related to the multiple scattering angle θ_0 by formula [4]:

$$\theta_0 = \frac{13.6 MeV}{\beta p}\sqrt{\frac{t}{X_0}}[1 + 0.038\ log(\frac{t}{X_0})] \qquad (1)$$

is not actually used by the Monte Carlo realisation of the Molière theory in GEANT (as it is very well explained in [2]) due to the fact that the scattering angles through consecutive small steps do not add up in quadrature in this theory. Instead, GEANT Monte Carlo calculates the scattering angle θ_0 through a given material step t according to detailed parametrisations of the exact Molière theory, corrected for finite angle scattering as described by Bethe. These parametrisations depend only on the quantities specified in the first four columns in tables 1 and 2, apart from pion energy and velocity.

For the sake of comparison with other approaches, one may however wish to make the approximation of obtaining an equivalent radiation length X_0 from the effective A, Z and ρ input values given to GEANT-DIRAC in tables 1 and 2. In order to do so, we may use for example the formula due to Dahl [4]:

$$X_0 = \frac{716.4 gcm^{-2} A}{Z(Z+1)log(287/\sqrt{Z})\rho} \qquad (2)$$

and the result of this exercise is indicated in the last two columns of tables 1 and 2, where the values of X_0 and X_0 % fraction (corresponding to real

thickness) are given for each tracking medium. Following this approximation, a total radiation length can be obtained by adding the contributions of individual layers in each MSGC and SFD detector, which is also presented in the last raw [1].

The vertex resolution falls short with these parameters with respect to the one observed with real data, as illustrated in figures 2 and 3. The difference is very appreciable.

The most obvious interpretation for this difference is that the average radiation length fraction for upstream detectors is underestimated by the Monte Carlo. In fact, the data were provided by detector builder groups, and most of the materials are composites for which chemical composition is uncertain with accuracy better than 10-20%. In addition, the list of small components in GEANT is never complete, and approximations have been made to simplify the geometry. On the other hand, both purity and thickness of the 94μm target foil were subject to specific controls, so we did not assume that they should be changed. In any case, our analysis was restricted to the 94 μm data sample (in correspondance with the Monte Carlo input), leaving aside the 98 μm data. We do not include the Ionisation Detector (IH) in this particular definition of upstream detectors, since obviously it cannot be responsible for the discrepancy, being located past the SFD.

In order to check whether this hypothesis is correct, we have increased the average multiple scattering angle , which we call $\bar{\theta}_0$, in all upstream detectors (excluding the target foil, which is well measured) by 12%, 13.5%, 15%, 16.5%, 18% 19.5% and 21%, and re-processed all GEANT-DIRAC tracking . The output for every dataset (40 buffer files of 50K events each) is available for use by ARIANE, so that detector digitisations and/or reconstruction procedures may be easily changed afterwards.

A good description of the data is in fact achieved by the Monte Carlo with 15% increase in $\bar{\theta}_0$, both in normalisation and in momentum derivative, as it is illustrated in figures 2 and 3. In fact, in order to measure the agreement between each Monte Carlo hypothesis of $\bar{\theta}_0$ and the prompt data, a χ^2 has been defined as:

$$\chi^2 = \sum_i \frac{\left(\sigma_p^i - \sigma_{MC}^i\right)^2}{\left(\Delta\sigma_p^i\right)^2 + \left(\Delta\sigma_{MC}^i\right)^2} \tag{3}$$

[1] these one-detector values (55.45×10^{-4} for MSGC and 83.79×10^{-4} for SFD-X) can be compared with those obtained in reference [6], namely 53.86×10^{-4} for MSGC and 83.36×10^{-4} for SFD-X, with a specific definition of equivalent X_0, outside the GEANT framework. Comments about this result will follow in section 6.

where i runs over 7 bins of track momentum in each projection (X or Y). The evolution of χ^2 as function of $\Delta\bar{\theta}_0/\bar{\theta}_0$ is shown in figure 4 for X and Y projections separately. Note that $\Delta\bar{\theta}_0/\bar{\theta}_0$ indicates the relative change in the mean multiple scattering angle $\bar{\theta}_0$ with respect to the nominal (0%) values indicated in tables 1 and 2.

A minimum χ^2 (after parabolic interpolation) is found in X projection at approximately +16.5% and +14.5% in Y. A systematic error is estimated in $\pm$ 1.5% from the figures, and from the relative consistency between both projections. This point will be confirmed by the studies made in the following section. It applies to a mean observed deviation of +15%.

The vertex distributions for the best Monte Carlo fit are also compared in figure 1 with real prompt data, and excellent agreement is found. Although maximum and minimum momentum bins were chosen for illustration, agreement is equally good in all momentum bins.

Let us clearly point out that this Monte Carlo corresponds to the standard $\pi^+\pi^-$ Coulomb-correlated generator input, as it is used for the lifetime analysis, where a good description of Q_T and Q_L is essential.

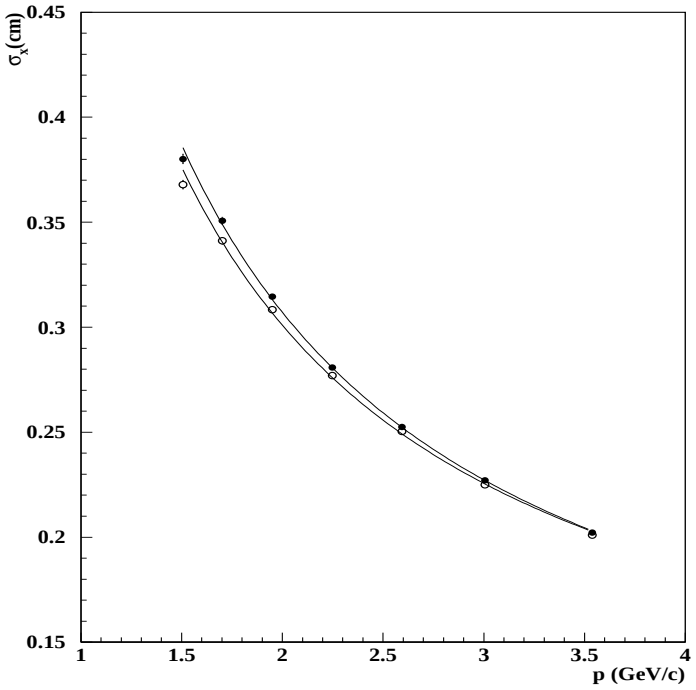

Fig. 5. *Comparison between the vertex resolution in X projection obtained from fitting methods A (full circles) and B (open circles) described in the text. Detector resolutions were 260 μm for SFD and 116μm for MSGC.*

3 Checks on systematic effects

Let us now review other aspects of the GEANT-DIRAC Monte Carlo simulation and reconstruction, apart from the upstream radiation length fraction, that might be unrealistic and could perhaps explain the observed deficit in vertex resolution.

3.1 Track fitting procedure

The vertex resolution deficit observed with the standard GEANT-DIRAC Monte Carlo does not depend on the particular choice of track fitting procedure that it is adopted. In fact, there are two (ARIANE selectable) mathematical procedures that have been used:

A) simple straight-line fit
B) multiple scattering correlated fit

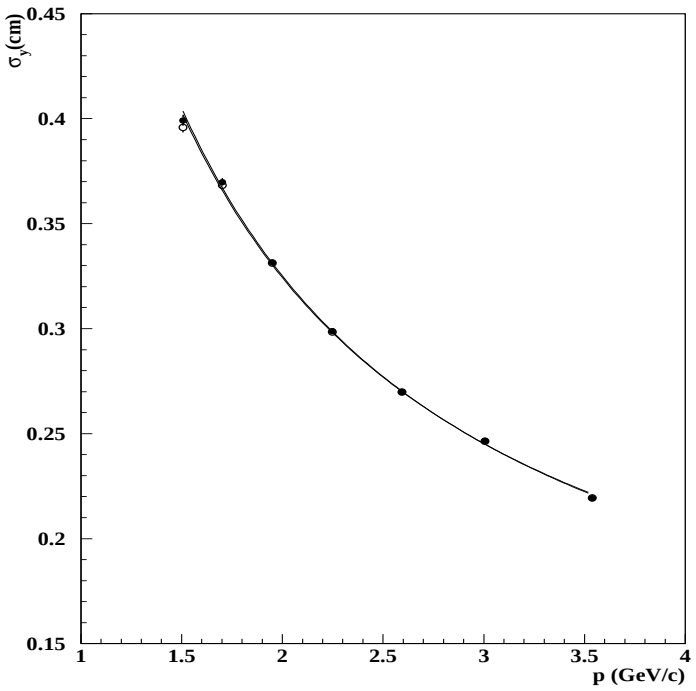

Fig. 6. *Comparison between the vertex resolution in Y projection obtained from fitting methods A (full circles) and B (open circles) described in the text. Same conditions as in figure 5.*

Both of them perform a least-squared method to minimize the track χ^2, and are described in detail in reference [1]. In method A, the detector covariance

matrix consists of only diagonal terms, namely the inverse of the squared intrisic resolutions of the 7 upstream detectors (6 in 2001 configuration). In method B, momentum-dependent non-diagonal terms are added in order to describe multiple scattering correlations between detector elements, as well as diagonal terms describing particle propagation through multiple thin layers. In both of them, detector resolutions are input to the program, and need to be known "a priori". As we shall see, the fitted track parameters depend on those only at second order.

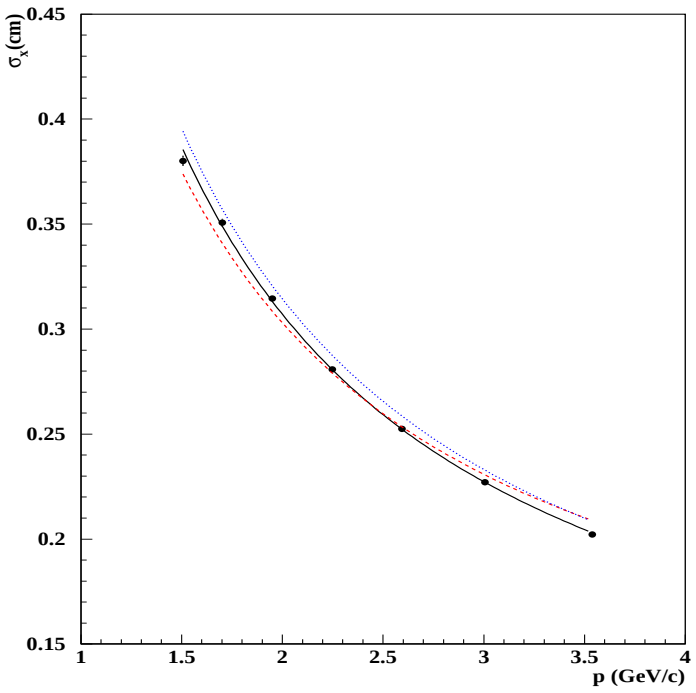

Fig. 7. *Comparison between vertex resolution obtained (in method A) from different hypothesis for the ratio of detector resolutions* $\sigma_{sfd}/\sigma_{msgc}$ *namely 2 (line). 4 (dashed) and 1 (dotted).*

The fit results are (in both cases) insensitive to an overall covariance matrix normalization factor. As a consequence, in method A a global scale factor on the MSGC and SFD resolution hypothesis is irrelevant. Only the ratio between the two is significant, which is approximately given by a factor 2, according to their respective pitch distances. In method B, the radiation length fractions of individual detector elements are given as input for the correlation matrix (values indicated in reference [7] were used for this purpose), as well as particle momenta determined by ARIANE event by event.

Figures 5 and 6 show a comparison between vertex resolution obtained with methods A and B, for the same hypothesis of detector resolution, in X and Y projections respectively. One can see that the differences between the two methods are small, due to the fact that in a given projection there are only 3

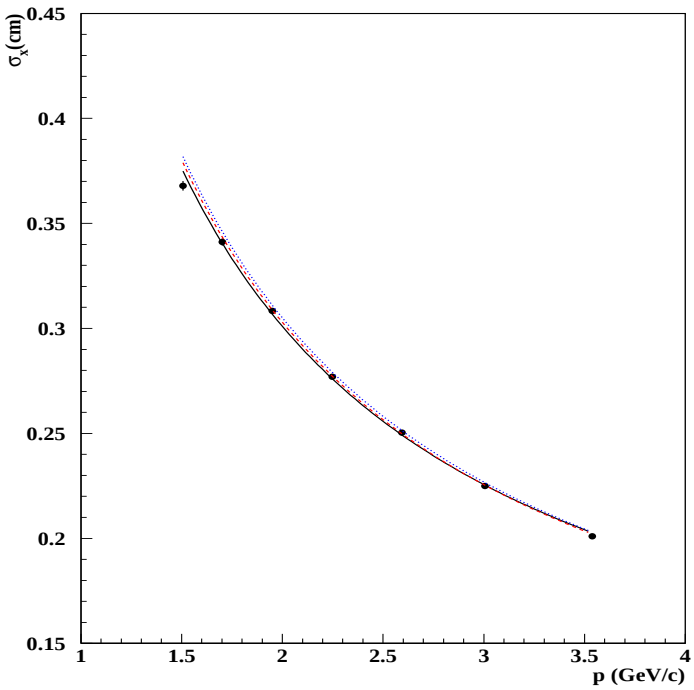

Fig. 8. *Comparison between vertex resolution (X-projection) obtained in method B from different scale factors on overall radiation length detector fractions in covariance matrix. Continuous line and full circles corresponds to the standard setting, dotted line to scale factor 1.5 and dashed line to scale factor 0.5 (note scattering angle scales with the square).*

effective detectors subject to correlation (for example, $X, X^{'}, SFD-X$), which is the minimum in order for the formalism to be effective. Method B simply provides a slightly better resolution at low momentum, better appreciated in X.

Now figure 7 shows the effect of changing the ratio $\sigma_{sfd}/\sigma_{msgc}$ from 1 to 4 in method A, and figure 8 the effect of changing the average radiation length in all detector layers by $\pm$ 50 %, in method B (leaving detector resolutions unchanged). Both changes are very extreme (by far inconsistent with our knowledge of those parameters), but nevertheless their impact on vertex resolution is minor.

In summary, it has been shown that differences due to the tracking procedure are themselves smaller that the observed resolution deficit, therefore it is excluded that they could explain it. Although we reported here (for brevity) the results obtained with real spectrometer data, we observe exactly the same trend with Monte Carlo data.

After consideration of the previous results, we have adopted method A as the baseline for our analysis, consistently throughout this note. Clearly the issue is not having the best resolution, but rather being more sensitive to multiple scattering and insensitive to tracking details, particularly when the amount of matter is itself subject to evaluation.

3.2 MSGC clusterisation

The second aspect of Monte Carlo simulation that we have analysed in detail is whether MSGC ARIANE digitisations (i.e. cluster strip multiplicities and charges) might be wrongly simulated. In other words, whether the description of detector resolution parameters of MSGC might influence the results. Of course, it is quite clear that with a single-hit resolution of 50μm [7] this influence is bound to be small as compared to multiple scattering, given the detector geometry. In any case, here again the Monte Carlo is severely constrained by the real data which are used as input.

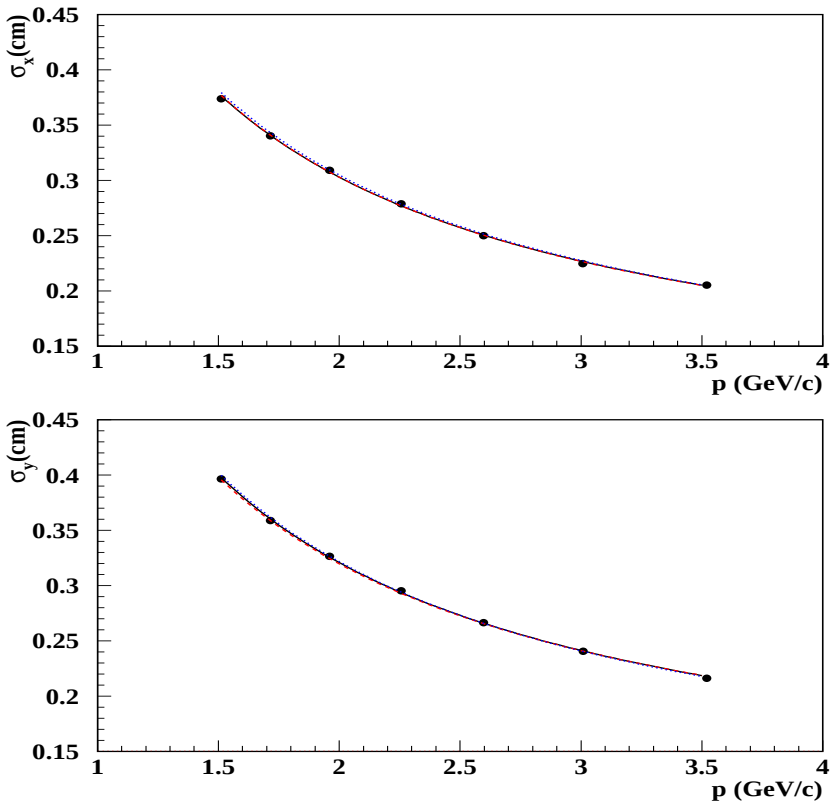

Fig. 9. *Comparison between vertex resolution obtained after variation of the MSGC cluster size shown in figure 10. The full circles and line correspond to the standard digitisation, where real multiplicity is simulated. Dotted/dashed lines are obtained with all clusters having one/two microstrips only.*

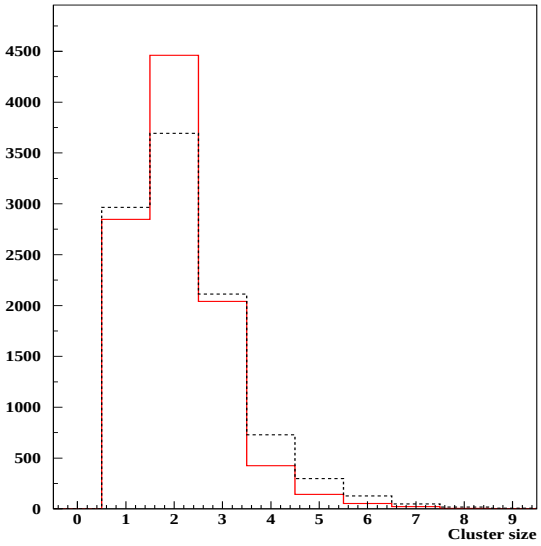

Fig. 10. *Distribution of microstrip multiplicity (cluster size) of MSGC hits in real 2001 data. Black dashed line includes background hits, whereas red line only those that belong to tracks.*

For illustration, we show in figure 9 the prediction for vertex resolution under the assumption that all cluster sizes were equal to one microstrip and that all were equal to two microstrips. The microstrip multiplicity distribution is indicated in figure 10. It is clear that both asumptions are extreme, in relation with the precision of the digitisation code. However, the changes induced are very small.

The conclusion of this study is that strong variations in the intrinsic resolution of MSGC cannot explain the observed discrepancy in vertex resolution, and hardly change the Monte Carlo prediction.

3.3 MSGC background

Noise level is quite strong in both MSGC and SFD detectors. Because the vertex resolution relies mostly on the MSGC, we have studied the influence of changing the MSGC background conditions on the previous results.

The general characteristics of MSGC background are described in reference [8], together with the simulation tools used. It is important to note that this simulation is totally constrained by the observed hit multiplicities. We show in figure 11 (bottom part) the number of MSGC hits found within a 3σ road around drift chamber tracks, for each detector plane, together with Monte Carlo simulation. The full 2001 data sample is included, in order to account for

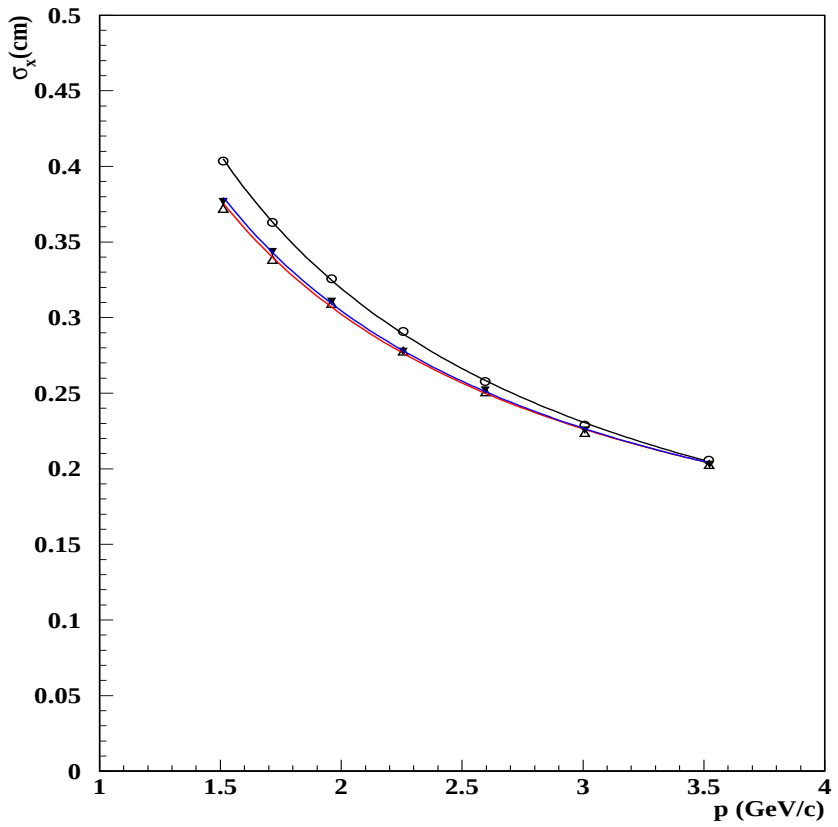

Fig. 11. *Comparison between vertex resolution (X-projection) obtained after variation of MSGC background level. Open/full triangles indicate +/- 10% variation of MSGC average hit multiplicity, with respect to the observed (standard) values in figure 12. Open circles show the case where MSGC background is totally removed (lines are also shown in all cases, following a fit to* $a + b/p$ *parametrisation).*

possible run-to-run variations. As it can be appreciated, the simulation quality is excellent. Not only average values are described, but also multiplicity shape is correctly reproduced.

We show in figure 11 the vertex resolution obtained after $\pm$ 10% variation of average hit multiplicity, as compared with the observed average values. For reference, we also show the prediction for null MSGC background. It is clear that significant changes on noise conditions hardly change the result. The extreme hypothesis of null background clearly illustrates the effect of noise. At low momentum (where search windows are larger for multiple scattering), the probability for noise hits to enter the track is higher, given the fact that pattern recognition uses the calibrated beam spot center. Therefore, the vertex resolution becomes artificially improved.

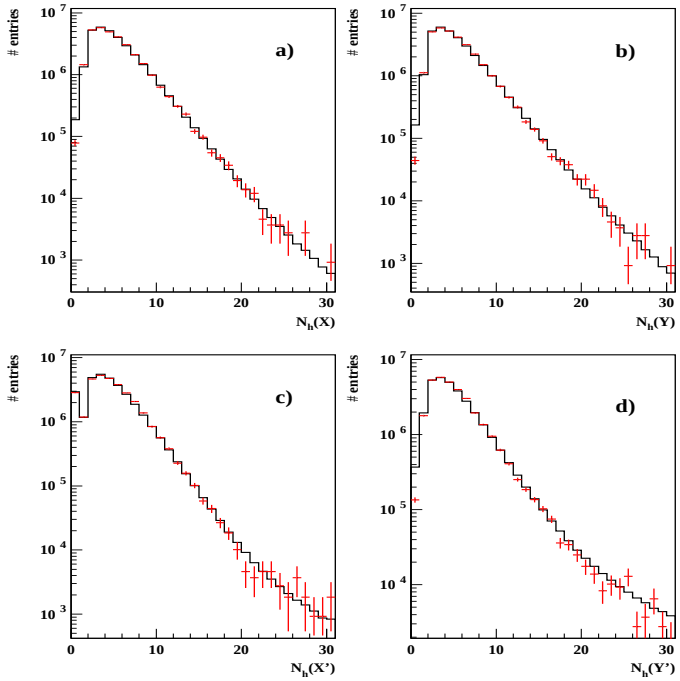

Fig. 12. *Real MSGC hit multiplicity distributions for each detector in 2001 data (full histogram), along with standard Monte Carlo simulation (crosses).*

We conclude that a wrong simulation of MSGC background does not significantly change the observed deficit in vertex resolution.

3.4 SFD background

In figure 13 we show the vertex resolution obtained with SFD background removed, as compared with the one with nominal parameters. Although the background level (under control of ARIANE via flux and cross-talk parameters) is high, its influence on vertex resolution is negligible (both in X and Y). This is understood, since noise SFD hits will not be followed by MSGC hits in front, and the track will not be reconstructed (let us recall that 6-hit tracks were selected in this analysis).

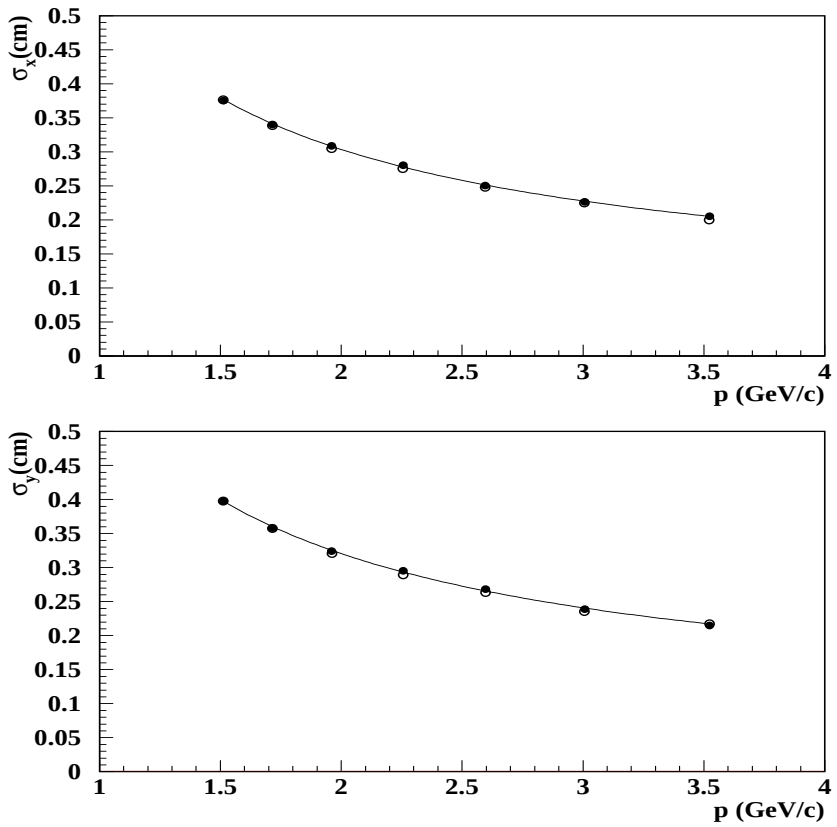

Fig. 13. *Comparison between vertex resolution in X (top) and Y (bottom) obtained from standard simulation (full circles) and simulation with SFD background removed.*

3.5 Beam spotsize and accidental pairs

In order to make an accurate comparison between spectrometer data and $\pi^+\pi^-$ Monte Carlo, we have corrected the prompt experimental data to account for the approximately 10% background of accidental pairs which can be determined from observation of the precision time-of-flight spectrum. In fact, vertex resolution (determined by the MSGC's) is sensitive to the presence of fluctuations of track origin within the beam dimensions, as they are expected to happen with accidental pairs. This is illustrated in figure 14, where prompt pairs are compared with accidentals. The difference is more significant in the vertical projection, where the beam dispersion is significantly larger.

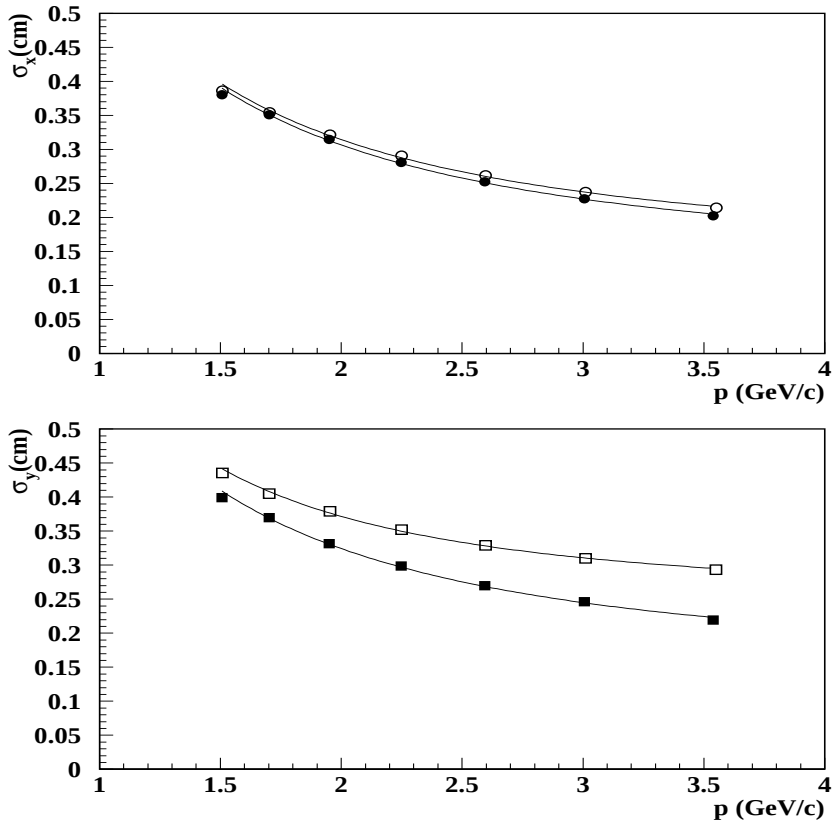

Fig. 14. *Comparison between vertex resolution observed for prompt pairs (black) and accidental pairs (open) of 2001 data period. Top figure refers to X-projection and bottom figure to Y-projection.*

In the results presented so far, a 10% fraction of the observed vertex distribution for accidental pairs was subtracted bin-by-bin from the prompt distribution, before the Gaussian fit is done, at every momentum interval. The actual effect of this subtraction is quite small, even in vertical projection. It should be recalled that only the central part of the vertex distribution is fitted to a

Gaussian (see figure 2). We have cross-checked that the observed behaviour with real data is indeed well understood by a specific Monte Carlo made for accidental pairs, where the beam dimensions can be changed.

The beam spotsize can be determined however using only experimental data, by fitting the points in figure 14 to the expression $\sigma_{x,y} = \sqrt{A_{x,y}^2 + B_{x,y}^2/p^2}$, where the $A_{x,y}$ parameter represents momentum-independent fluctuations (detector resolution and beam size), and the $B_{x,y}$ parameter those from multiple scattering. By taking the differences $\sqrt{A_{acc}^2 - A_{prompt}^2}$ we can estimate the beam dimensions, and the results are indicated in table 3. They are in reasonable agreement with those of reference [9]. It is remarkable that, despite the strong variation from A_x to A_y for accidental pairs (due to beam width), the values of B_x and B_y are hardly different, as expected. Note the data cover the full 2001 data period with Ni 24 GeV/c beam.

Table 3
Fitted values for A and B from prompt and accidental pairs, and beam spot sizes σ_x and σ_y determined from A parameters. Note that only statistical errors are quoted here.

	A_x (cm)	B_x (cm·GeV/c)	A_y (cm)	B_y (cm·GeV/c)
Prompt	0.133 ± 0.002	0.552 ± 0.003	0.154 ± 0.002	0.570 ± 0.003
Accidentals	0.150 ± 0.002	0.552 ± 0.003	0.252 ± 0.001	0.547 ± 0.003

σ_x (cm)	σ_y (cm)
0.069 ± 0.005	0.204 ± 0.002

3.6 Long lifetime particles

The strong time coincidence, achieved with precision time-of-flight counters for prompt pairs, may still correlate pion pairs from the same proton interaction, where one of them is actually the decay product of another particle, with delay shorter than 0.9 *ns*. It is in principle possible that those long-lifetime decays (no larger than 10% , as determined by the pionium analysis program) gave a wider transverse vertex distribution, and that this effect might be the explanation of the resolution shortfall.

We have made a simple check, by selecting only pairs where one of them has a muon tag, determined by the coincidence of muon counters and pre-shower detector signals. The vertex resolution from those events (100% muon tagged) is compared with the standard one from prompt pairs (where muon tagged

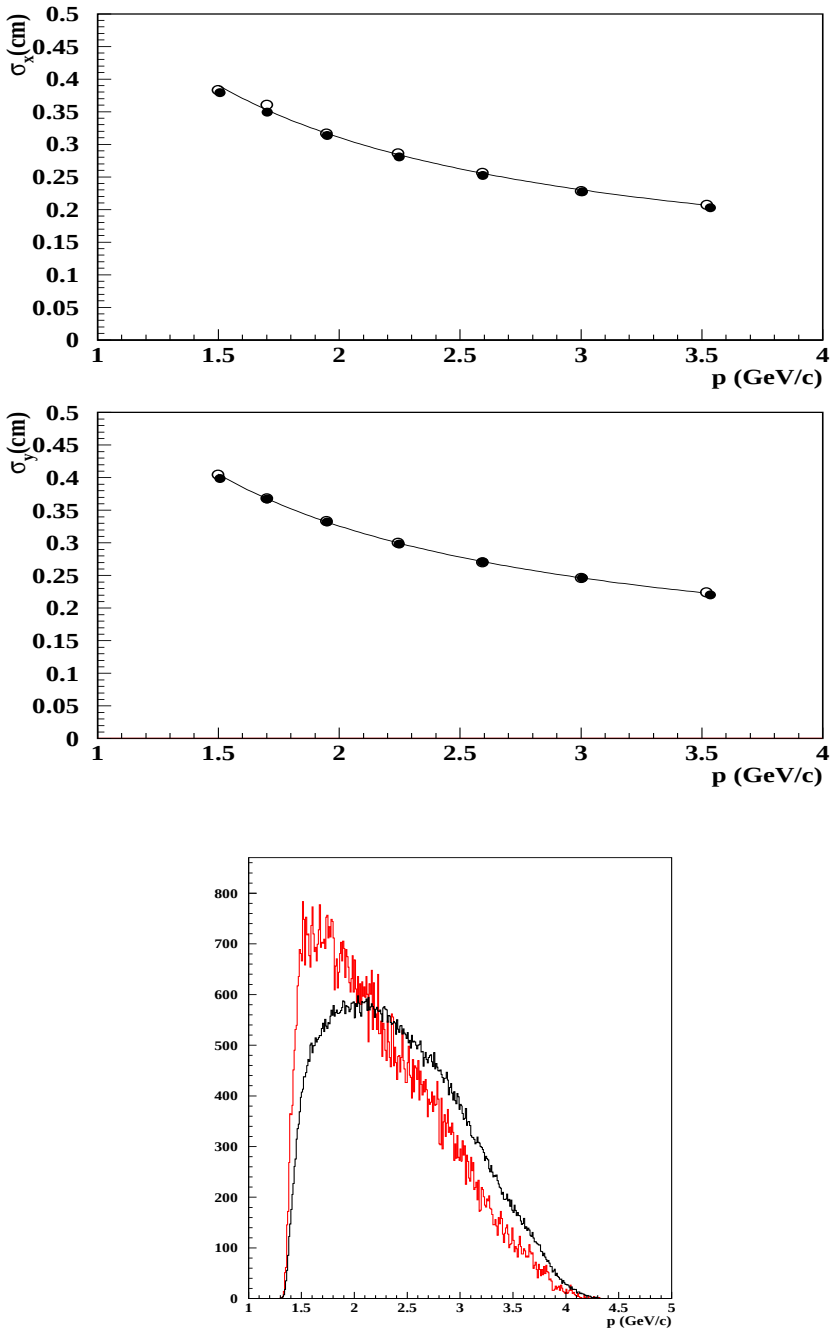

Fig. 15. *Comparison between vertex resolution observed with prompt pairs having muon tags removed (full circles) and pairs with only muon tags (open circles). X and Y projections are shown separately. The bottom figure shows the momentum spectra for the corresponding prompt (black) and muon-tagged (red) pairs, with equal normalisation.*

events were vetoed) and it is shown in figure 15. The observed muon fraction (rejected by standard ARIANE reconstruction) is about 10%, in agreement

with expectation, and the lab momentum spectra are compared in figure 15, showing a softer muon spectrum, probably due to neutrino emission. Despite the fact that pion lifetime is larger than any other possible long-lifetime resonance contribution, the vertex distribution is hardly distorted in the tranverse direction. Note should be taken that the $Q_T < 4MeV/c$ cut avoids large-angle tracks by construction, no matter how large the resonance mass can be. So it is clear that a possible explanation of resolution deficit by long-lifetime decays can be safely excluded.

4 Conclusions

The following conclusions can be derived from the analysis presented in this note:

1) The average multiple scattering angle in upstream detectors is underestimated by standard GEANT-DIRAC Monte Carlo by 15 $\pm$ 1.5 % . Wrong values were therefore used as the baseline analysis for DIRAC lifetime publication [10], which needs to be revised, both for real values and for systematic error analysis. The results agree with our presentation to the collaboration made on February 19. We find no other possible interpretation of the vertex resolution data analysed here.
2) Measurements of multiple scattering angle from a dedicated setup using drift chambers have been reported [6]. We did not find in this publication a direct comparison with GEANT-DIRAC Monte Carlo for the detectors under test, but rather a determination of an equivalent radiation length based upon a three-Gaussian fit [2] . Since this is far from being the approach followed by GEANT, we see no way to derive conclusions from the approximate equality of the equivalent radiation lengths found in [6] for MSGC and SFD-X and those quoted in tables 1 and 2. Apart from the fact that the usual radiation length fraction concept, as illustrated for example in formula (1), is not used in any of the two approaches, the definition of *equivalent* is different: in one case, it arises from the three-Gaussian fit, and in the other from utilisation of Dahl's formula (2), actually outside the GEANT tracking framework.
3) We find no sign of poor performance of GEANT-DIRAC tracking, using Molière-Bethe theory, after having rescaled the average multiple scattering angle in upstream detectors. On the contrary, after this rescaling (which is mathematically equivalent to a redefinition of average A,Z and/or small thickness or geometry changes), the performance is really good in all critical

[2] it is interesting to remark that this equivalent radiation length of pure elements like Ni and Al are larger than those reported by the Particle Data Group [4] by factors 1.15 and 1.20, respectively.

distributions such as momentum and opening-angle dependence of vertex resolution. This is the simplest and most effective solution, since what the DIRAC experiment needs is an accurate description of Q_T resolution in $\pi^+\pi^-$ phase space, and this goal is fully achieved, as it has been demonstrated.

References

[1] DIRAC note 03-08, *A Tracking System for Upstream Detectors in DIRAC*, B. Adeva, A. Romero and O. Vázquez Doce.

[2] *GEANT - Detector Description and Simulation Tool* http://wwwasdoc.web.cern.ch/wwwasdoc/geant_html3/geantall.html

[3] DIRAC note 98-08, *The GEANT-DIRAC Simulation Program Version 2.5. P. Zrelov and V. Yazkov.* http://zrelov.home.cern.ch/zrelov/dirac/montecarlo/instruction/instruct26.html

[4] Particle Data Group, Phys. Rev. D66 (2002) 010001.

[5] B. Rossi and K. Greisen, Rev. Mod. Physics, 13:240, 1941.

[6] DIRAC note 05-02, *Pion multiple Coulomb scattering in the DIRAC experiment.* A. Dudarev, V. Kruglov, L. Kruglova, M. Nikitin

[7] B. Adeva et al., *DIRAC : A High Resolution Spectrometer for Pionium Detection*, Nucl. Inst. and Meth. A515 (2003) 467-496.

[8] DIRAC note 05-11, *Study of SFD efficiency using MSGC detector for 2001 data*, B. Adeva, A. Romero, O. Vázquez Doce

[9] DIRAC note 02-02, *DIRAC beam parameters* A. Lanaro.

[10] B.Adeva et al., *First measurement of the pi+ pi- atom lifetime*, Physics Letters B 619 (2005) 50.